
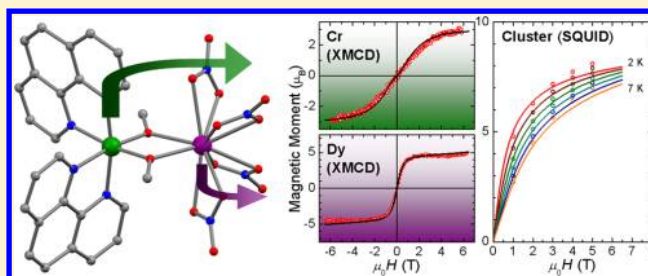


X-ray Magnetic Circular Dichroism (XMCD) Study of a Methoxide-Bridged Dy^{III}–Cr^{III} Cluster Obtained by Fluoride Abstraction from *cis*-[Cr^{III}F₂(phen)₂]⁺Jan Dreiser,^{*,†} Kasper S. Pedersen,[‡] Torben Birk,[‡] Magnus Schau-Magnussen,[‡] Cinthia Piamonteze,[†] Stefano Rusponi,[§] Thomas Weyhermüller,[#] Harald Brune,[§] Frithjof Nolting,[†] and Jesper Bendix^{*,‡}[†]Swiss Light Source, Paul Scherrer Institut, CH-5232 Villigen PSI, Switzerland[‡]Department of Chemistry, University of Copenhagen, DK-2100 Copenhagen, Denmark[§]Institute of Condensed Matter Physics, Ecole Polytechnique Fédérale de Lausanne, CH-1015 Lausanne, Switzerland[#]Max Planck Institute for Bioinorganic Chemistry, D-45470 Mülheim an der Ruhr, Germany Supporting Information

ABSTRACT: An isostructural series of dinuclear chromium(III)–lanthanide(III) clusters is formed by fluoride abstraction of *cis*-[CrF₂(phen)₂]⁺ by Ln³⁺ resulting in LnF₃ and methoxide-bridged Cr–Ln clusters (Ln = Nd (1), Tb (2), Dy (3)) of formula [Cr^{III}(phen)₂(μ-MeO)₂Ln(NO₃)₄]*x*MeOH (*x* = 2–2.73). In contrast to fluoride, methoxide bridges in a nonlinear fashion, which facilitates chelation. For 3, X-ray magnetic circular dichroism (XMCD) provides element-specific magnetization curves that are compared to cluster magnetization and susceptibility data acquired by SQUID magnetometry. The combination of XMCD and SQUID is able to resolve very small magnetic coupling values and reveals a weak Cr^{III}–Dy^{III} coupling of $j = -0.04(3) \text{ cm}^{-1}$. The Dy^{III} ion has a ground-state Kramers doublet of $m_j = \pm 13/2$, and the first excited doublet is found to be $m_j = \pm 11/2$ at an energy of $\delta = 57(21) \text{ cm}^{-1}$. The Cr^{III} ion exhibits a uniaxial anisotropy of $D_{\text{Cr}} = -1.7(1.0) \text{ cm}^{-1}$. Further, we observe that a weak anisotropic coupling of dipolar origin is sufficient to model the data, suggesting that methoxide bridges do not play a significant role in the magnetic coupling for the present systems.

**■ INTRODUCTION**

Molecular nanomagnets¹ have attracted a lot of interest because of their fascinating properties and their prospects in future applications in quantum information processing and molecular spintronics.² In particular, there is increasing activity regarding 3d–4f single-molecule magnets, and numerous species have been reported so far.^{3,4} The complete understanding of their magnetic behavior is, however, lagging behind, and for instance, the key to the necessary ingredients that mediate properties such as slow relaxation of magnetization in 3d–4f clusters is still missing.⁵ Difficulties in finding this key are aggravated by the complexity of the magnetism of 4f ions with orbital contribution to their ground state.⁶ In particular, it is difficult to obtain precise values of the magnetic exchange coupling between 3d and 4f ions: In 3d clusters, this information can be readily extracted from dc magnetic susceptibility measurements; however, the large anisotropy splittings resulting from the 4f ligand-field states can strongly influence the temperature dependence of the magnetic susceptibility. Hence, exchange coupling deduced solely from susceptibility data may be subject to large uncertainties. The problem can be circumvented by using additional methods such as diamagnetic substitution,^{7,8} electron paramagnetic resonance,⁸ or inelastic neutron

scattering studies.⁹ X-ray magnetic circular dichroism¹⁰ (XMCD) is able to obtain absolute values of element-specific magnetization, which can in turn be exploited to obtain a sensitive measurement of very small magnetic coupling values, and thus it is among the techniques of choice to quantify such coupling in 3d–4f clusters.¹¹ Precise knowledge about the magnetic exchange coupling is the prerequisite for obtaining its dependence along the homologous series of lanthanides and for establishing magneto-structural correlations,^{3a,12} and thus it is of importance for the rational design of polynuclear 3d–4f complexes. The recent detailed studies of 3d–4f magnetic interactions have revealed a number of nonisotropic interaction modes such as anisotropic or antisymmetric interactions. Disregarding the interaction mode, most studies have reported weak 3d–4f interactions ($j_{3d-4f} < 1 \text{ cm}^{-1}$). However, also for systems with weakly interacting magnetic centers and concomitant high ground-state degeneracies, the quantification of the interaction strength is important. Such systems are receiving rapidly growing interest due to their large magneto-

Received: April 12, 2012

Revised: June 26, 2012

Published: July 12, 2012

caloric effects and potential applications in magnetic refrigeration.¹³ Recently, we reported the first examples of 3d–4f clusters assembled by unsupported fluoride bridges.^{11b,14} Here we report the synthesis and the structural characterization of a novel series of methoxide-bridged clusters: $[\text{Cr}^{\text{III}}(\text{phen})_2(\mu\text{-MeO})_2\text{Ln}(\text{NO}_3)_4] \cdot x\text{MeOH}$ with Ln = Nd (**1**), Tb (**2**), and Dy (**3**). As for the previously reported, fluoride-bridged systems, the chromium precursor in the present study is the robust *cis*- $[\text{Cr}^{\text{III}}\text{F}_2(\text{phen})_2]^+$ ion. However, instead of targeting the kinetic product in the form of tetranuclear $[\{\text{CrF}_2(\text{phen})_2\}_2\{\text{Ln}(\text{NO}_3)_4\}_2]$ squares, we have found that the reaction can be driven more toward thermodynamic products, by use of more dilute solutions and longer reaction times. The approach relies on the high affinity of the lanthanides for fluoride, which leads to eventual abstraction of fluoride from the Cr(III) precursor complex and introduction of solvent-derived bridges. This may constitute a generalizable synthetic approach to systems with alkoxide-bridged lanthanide clusters, some of which have recently been shown to possess SMM properties with relatively high relaxation barriers.¹⁵ For **3** a detailed magnetic study involving XMCD and SQUID magnetometry has been employed to characterize the exchange coupling and magnetic anisotropies.

EXPERIMENTAL SECTION

Synthesis. *cis*- $[\text{CrF}_2(\text{phen})_2]\text{NO}_3$ was prepared according to the literature.^{14a} $\text{Ln}(\text{NO}_3)_3\text{aq}$ and methanol were obtained by commercial sources (Alfa Aesar and Lab Scan HPLC, respectively) and used without further purification.

General Synthesis of $[(\text{phen})_2\text{Cr}(\mu\text{-CH}_3\text{O})_2\text{Ln}(\text{NO}_3)_4]$ (Ln = Nd (1**), Tb (**2**), Dy (**3**)).** All complexes were prepared at room temperature by slow diffusion of methanol solutions of the two reactants. The synthesis was carried out in a custom-made diffusion cell consisting of three consecutive chambers separated by two porous glass frits (No. 4). Each chamber has a volume of approximately 20 mL and can be sealed. In the two outer chambers solutions of *cis*- $[\text{CrF}_2(\text{phen})_2]\text{NO}_3$ (0.6 mmol) in MeOH (20 mL) and $\text{Ln}(\text{NO}_3)_3\text{aq}$ (0.6 mmol) in MeOH (20 mL) were placed, respectively, whereas the middle chamber was filled with methanol. The diffusion cell was sealed and left undisturbed until no visible changes in the cell were observed over a period of 3 months (total time of synthesis: 6–12 months). During this time of crystallization, large red crystals together with a fine white powder were formed in all three chambers. In the chamber where *cis*- $[\text{CrF}_2(\text{phen})_2]\text{NO}_3$ was originally placed, the white byproduct dominated considerably and the content of this chamber was discarded. The red crystals from the remaining chambers were harvested by gentle scratching with a spatula and repeatedly washed by decantation with methanol. This procedure directly gave crystals suitable for single crystal diffraction. (**1**): yield, 0.141 g (46.1% of theoretical based on Nd^{III}). Slightly lower yields were obtained for **2** and **3**. Elemental analysis calcd (%) for $\text{H}_{22}\text{C}_{26}\text{N}_8\text{O}_{14}\text{CrNd}$ (dried) (**1**): H, 2.30; C, 35.58; N, 12.51. Found (%): H, 2.33; C, 35.16; N, 12.39. Elemental analysis calcd (%) for $\text{H}_{22}\text{C}_{26}\text{N}_8\text{O}_{14}\text{CrDy}$ (dried) (**3**): H, 2.51; C, 35.29; N, 12.66. Found (%): H, 2.2; C, 34.7; N, 12.3.

Crystallography. Single crystals for X-ray structure determination were obtained by the synthetic procedure outlined above. Diffraction data for **1**, **2**, and **3** were collected with a Nonius KappaCCD area-detector diffractometer at $T = 122$ K (Oxford Cryostreams low-temperature device) employing Mo $K\alpha$ ($\lambda = 0.71073$ Å) X-rays. Structures were solved by

direct methods (SHELXS97) and refined with the SHELXL97 program package. Hydrogens were kept in fixed positions and all non-hydrogen atoms were treated anisotropically. Traces of cocrystallized methanol molecules were localized and the population refined. Crystallographic data are given in Table S1. CCDC-862729 (**1**), CCDC-862730 (**2**) and CCDC-862731 (**3**) contain the supplementary crystallographic data for this article. These data can be obtained free of charge from The Cambridge Crystallographic Data Centre via www.ccdc.cam.ac.uk/data_request/cif.

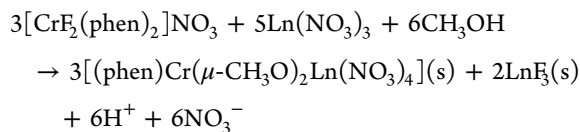
SQUID Measurements. All magnetic measurements were conducted on a Quantum Design MPMS-XL SQUID magnetometer. The crystalline sample was ground and mechanically immobilized in *n*-eicosane to avoid orientation effects. The magnetization was measured from 1.8 to 300 K in an applied dc field of $\mu_0 H_0 = 100$ mT. Reduced magnetization data were obtained at temperatures below 7 K in fields up to 5 T. Susceptibility was calculated using the relation $\chi = M/H_0$ and magnetization values were corrected using Pascal constants. The ac measurements utilized an ac field of $\mu_0 h_{\text{ac}} = 0.3$ mT with and without a static field (selected fields between 10 mT and 300 mT).

XMCD Measurements. X-ray absorption measurements were performed at the X-Treme endstation and beamline at the Swiss Light Source, Paul Scherrer Institut, Switzerland.¹⁶ X-ray absorption spectra were recorded on a powder sample of **3** at a temperature of 2 K in total electron yield mode. Magnetic fields of up to $\mu_0 H = \pm 6$ T along the beam direction were applied. The beam was defocused to a spot size of approximately 1×1 mm² and kept at very low intensity to exclude radiation damage. Photon-energy scans were recorded “on-the-fly”; that is, the monochromator and insertion device were moving continuously while the data were acquired.¹⁷ To measure magnetization curves, a full magnetic-field loop was performed at one circular polarization while X-ray absorption was measured at the energy of maximum dichroism and at the pre-edge. Then, the helicity of the X-rays was switched and another loop was run.

Spin-Hamiltonian Calculations and Fits. Element-specific and cluster magnetization curves as well as dc magnetic susceptibility were simulated by full diagonalization of Hamiltonian eq 1. Powder average over the magnetization curves and the susceptibility was calculated by use of a 16-point Lebedev-Laikov grid.¹⁸ All fits shown in this work are least-squares fits obtained by minimizing the sum of squared deviations between the measured and calculated curves. The calculations were performed using a home-written Matlab code.

RESULTS

Synthesis and Structural Analysis. Cr(III) complexes are generally kinetically robust due to the ligand-field stabilization of the octahedral d^3 configuration leading to frequent cases of isomerism and isolatable kinetic products. Here, we demonstrate that for fluoride complexes, this intrinsic robustness of Cr(III) complexes can be overcome by reaction with sufficiently strong fluoride acceptors such as lanthanide ions. Consequently, fluoride complexes are also viable and practical precursors for solvent-bridged polynuclear Cr(III)-4f systems. The one-to-one stoichiometric reaction of $\text{Ln}^{\text{III}}(\text{NO}_3)_3\text{aq}$ and *cis*- $[\text{CrF}_2(\text{phen})_2]^+$ in methanol produces $[\text{Cr}^{\text{III}}(\text{phen})_2(\mu\text{-MeO})_2\text{Ln}(\text{NO}_3)_4]$ over a time scale of months with the possible balanced reaction



The formation of $[(\text{phen})\text{Cr}(\mu\text{-CH}_3\text{O})_2\text{Ln}(\text{NO}_3)_4]$ is accompanied by a precipitation of a fine white powder. This, however, is easily removed by successive decantation. The powder is mainly lanthanide(III) fluoride as evidenced by powder X-ray diffraction and elemental analysis (see the Supporting Information). Lanthanide(III) fluorides are extremely insoluble owing to the very large lattice enthalpy. This fact complicates the isolation of fluoride bridged 3d–4f clusters and hence only very few examples are known.^{14,19}

Although alkoxide-bridged 3d–4f clusters are common, methoxide bridges are relatively rare, but the present approach might provide a generalizable approach to such systems.²⁰ All three members (1–3) are isostructural and crystallize in the orthorhombic *Pbcn* space group with $Z = 4$. Crystallographic data are given in Table S1 (Supporting Information). In 3, the bridging angle imposed by the methoxide ligands is Dy–O–Cr = $106.8(3)^\circ$ which is in the range of bond angles in similar systems.¹⁵ Other relevant bond lengths and angles are given in the caption of Figure 1. Interestingly, the chelation is opposed

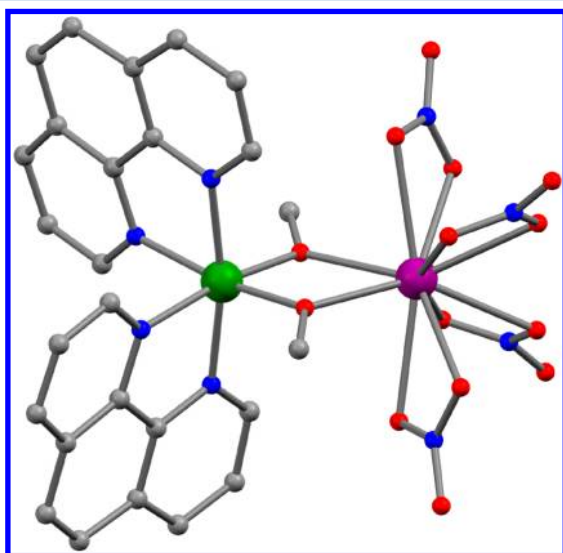


Figure 1. Ball-and-stick representation of 3. Color code: chromium, green; dysprosium, purple; nitrogen, blue; oxygen, red; carbon, gray. Hydrogens have been omitted for clarity. Selected bond lengths and angles: Dy–O_{MeO}, 2.324(6) Å; Dy–O_{NO₃}, 2.457(8)–2.528(6) Å; Cr–O, 1.921(6) Å; Cr–N, 2.064(7) Å, 2.076(7) Å; Cr–O–Dy, $106.8(3)^\circ$; O–Cr–O, $81.3(4)^\circ$; O_{MeO}–Dy–O_{MeO}, $65.2(3)^\circ$; Cr···Dy, 3.42 Å.

to 3d–4f systems with unsupported fluoride bridges. In 1 and 2, bond lengths and angles are only slightly different from those in 3 as given in the caption to Figure 1.

X-ray Absorption and X-ray Magnetic Circular Dichroism. Polarization-dependent X-ray absorption spectra (XAS) of 3 are shown in Figures 2a and 3a. They were recorded at 6 T and 2 K at the Cr $L_{2,3}$ and Dy $M_{4,5}$ edges, respectively. For both elements, the spectra are strongly dichroic, as reflected in the XMCD spectra shown in Figures 2b and 3b, indicating the presence of large magnetic moments.

The element-specific magnetization curves depicted in Figure 4a,b reveal that the magnetic moments of the Dy^{III} and Cr^{III}

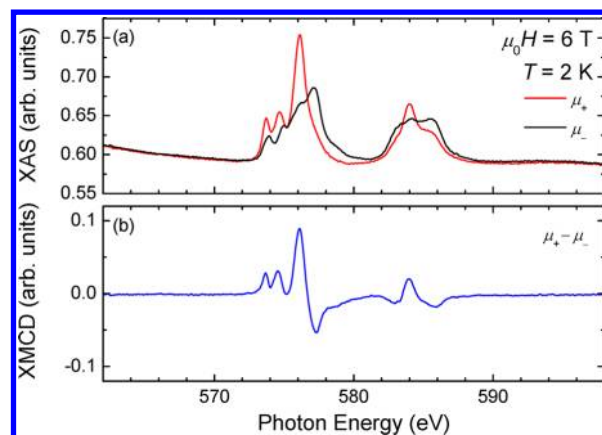


Figure 2. (a) XAS of 3 recorded at the Cr $L_{2,3}$ edges as a function of circular polarization. (b) XMCD spectrum obtained from the XAS shown in panel a.

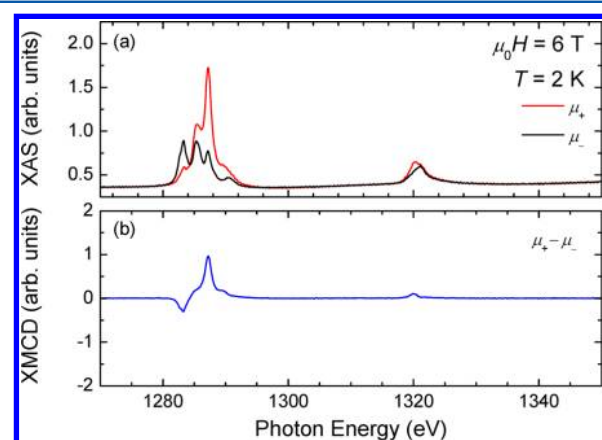


Figure 3. (a) Polarization dependent XAS of 3 recorded at the Dy $M_{4,5}$ edges as a function of circular polarization. (b) XMCD spectrum obtained from the XAS shown in panel a.

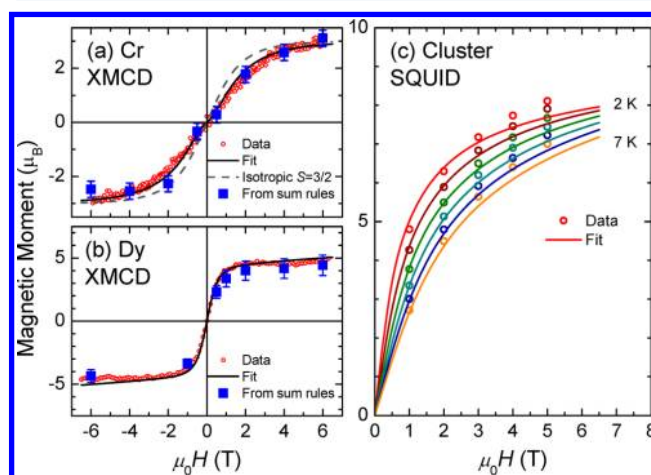


Figure 4. Element-specific magnetization curves for the Cr^{III} (a) and Dy^{III} (b) ions obtained on 3 by XMCD. The dashed line in (a) indicates the calculated magnetic moment for an isotropic $S = 3/2$ paramagnet using the Brillouin function. The squares mark the total (spin + orbital) magnetic moments obtained from sum rule analysis applied to couples $(\mu_+ - \mu_-)$ of spectra acquired at several H fields. (c) Cluster magnetization obtained by SQUID magnetometry. Solid lines in (a)–(c) indicate best-fit curves with parameters given in the text.

ions are always oriented parallel to the applied magnetic field. Blue squares in Figure 4 indicate the values of the total (spin and orbital) magnetic moments found by sum rule analysis²¹ assuming ion-like hole numbers, that is $N_{\text{eff}} = 7$ and $N_{\text{eff}} = 5$ for Cr^{III} and Dy^{III} , respectively. For Dy^{III} , the average ratio of orbital versus spin angular momentum was found to be $\langle L_z \rangle / \langle S_z \rangle = 1.8(2)$, in excellent agreement with the expected value of 2.0 from Hund's rules. Details of the sum rule analysis are given in the Supporting Information. The dashed line in Figure 4a represents the calculated magnetization of an isotropic paramagnet with $S = 3/2$ described by the Brillouin function.

SQUID Magnetometry. The cluster magnetization curves of **3** for temperatures of 2–7 K are plotted in Figure 4c. Clearly the magnetization does not reach saturation at the highest field of 5 T, indicating the presence of significant anisotropy and/or low-lying excited energy levels. The temperature-dependent dc magnetic susceptibility is plotted as χT product in Figure 5. At

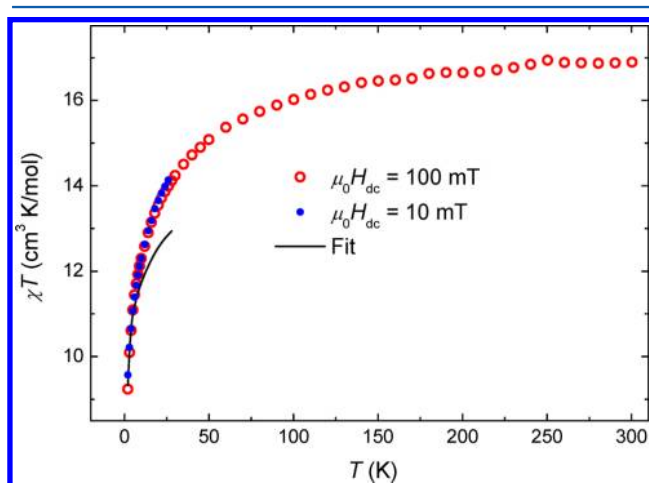


Figure 5. dc magnetic susceptibility of **3** shown as χT product. Circles correspond to the data, and the solid line is the best-fit curve obtained using the parameters given in the text. The deviation of the model curve from the experimental data at higher temperatures is a consequence of the restricted function space of the Dy^{III} ion used in the modeling (see text for a detailed Discussion).

room temperature $\chi T = 16.9 \text{ cm}^3 \text{ K mol}^{-1}$. From this value one can directly derive the sum of the magnetic moments per molecule, because the coupling between the magnetic ions is much smaller than the thermal energy at 300 K, and hence it plays no role. We find that this value is consistent with the presence of a Dy^{III} ion and a Cr^{III} ion in the cluster, which yields a theoretical value of $16.05 \text{ cm}^3 \text{ K mol}^{-1}$, using $g_{\text{Dy}} = 4/3$ and $g_{\text{Cr}} = 2$. Upon decreasing the temperature, the χT product drops moderately at intermediate temperatures and decreases steeply at low temperatures. Such behavior can arise from antiferromagnetic interactions within the cluster and/or the depopulation of the Dy ligand-field states. ac susceptibility measurements at $1.8 \text{ K} \leq T \leq 20 \text{ K}$ with and without a dc magnetic field revealed no out-of-phase (χ'') component excluding the possibility of slow magnetic relaxation and the presence of minor magnetic impurities of, e.g., DyF_3 .

Spin-Hamiltonian Model and Fits. To obtain quantitative information about magnetic exchange coupling and anisotropy in **3**, we have used a spin-Hamiltonian approach. Although the Cr^{III} ion can be modeled by a spin $S = 3/2$, the magnetic behavior of the Dy^{III} ion is more difficult to describe because of the orbital contribution to its magnetic moment. According to

Hund's rules, the ground-state multiplet of the Dy^{III} ion is $J = 15/2$ with the first excited multiplet separated by more than 4000 cm^{-1} . Owing to the ligand field the ground-state multiplet is split into eight Kramers doublets extending over an energy range of typically several hundreds of cm^{-1} . The wave functions and expectation values $\langle J_z \rangle$ of the ground-state doublet depend on the exact geometry and strength of the ligand field.^{22,23} To speed up calculations and more importantly to avoid overparametrization, we have restricted the basis set describing the Dy^{III} ion to the lowest two Kramers doublets. We have assumed collinear orientation of the Dy and Cr anisotropy axes, which is justified in the case of weak magnetic coupling. Further, we have assumed uniaxial anisotropies for both ions. This is certainly an approximation but we anticipate here that our rather simple model is able to reproduce our experimental data with a minimum number of fit parameters; hence it would not be reasonable to invoke a more complex model with additional free parameters. The spin-Hamiltonian operating on the restricted magnetic configuration space is given by

$$\hat{H} = -j\hat{\mathbf{J}}_{\text{Dy}} \cdot \hat{\mathbf{S}}_{\text{Cr}} + \left\{ D_{\text{Dy}} \left[\hat{J}_{\text{Dy},z}^2 - \frac{1}{3} J_{\text{Dy}} (J_{\text{Dy}} + 1) \right] + d_{\text{Dy}} \right\} + D_{\text{Cr}} \left[\hat{S}_{\text{Cr},z}^2 - \frac{1}{3} S_{\text{Cr}} (S_{\text{Cr}} + 1) \right] + \mu_{\text{B}} (g_{\text{Dy}} \hat{\mathbf{J}}_{\text{Dy}} + g_{\text{Cr}} \hat{\mathbf{S}}_{\text{Cr}}) \cdot \mathbf{B} \quad (1)$$

Here, $\hat{\mathbf{J}}_{\text{Dy}}$ and $\hat{\mathbf{S}}_{\text{Cr}}$ denote the total and spin angular momentum operators of the Dy^{III} and Cr^{III} ions, respectively, with $J_{\text{Dy}} = 15/2$ and $S_{\text{Cr}} = 3/2$. The first term represents an isotropic exchange coupling, the second and third terms are uniaxial anisotropies, and the last term is the interaction with the applied magnetic field. In the Dy anisotropy term, the parameters D_{Dy} and d_{Dy} are used to generate an energy splitting δ between the ground-state doublet and the first excited-state doublet while keeping the whole Dy anisotropy term traceless. This notation is of course valid in the restricted space only. The g -factors are taken to be isotropic and fixed to $g_{\text{Dy}} = 4/3$ (Landé g -factor) and $g_{\text{Cr}} = 2$. An isotropic Dy g -factor is justified because in eq 1 the $\hat{\mathbf{J}}_{\text{Dy}}$ operator has the property of a $15/2$ angular momentum, in contrast to an effective spin- $1/2$ model. However, the latter can be directly derived from the Hamiltonian eq 1.¹¹ The best-fit parameters and uncertainties are determined as

$$\begin{aligned} j &= -0.04(3) \text{ cm}^{-1} \\ D_{\text{Cr}} &= -1.7(1.0) \text{ cm}^{-1} \\ \delta &= 57(21) \text{ cm}^{-1} \\ m_{J,\text{GS}} &= \pm 13/2 \\ m_{J,\text{ES}} &= \pm 11/2 \end{aligned}$$

and the corresponding calculated element-specific and cluster magnetization as well as the χT product are plotted as solid lines in Figures 4 and 5. During the fitting process we have observed that there is a strong preference for the $m_{J,\text{GS}} = \pm 13/2$ ground-state doublet of the Dy^{III} ion. Regarding the first-excited state, the fits are slightly better with $m_{J,\text{ES}} = \pm 11/2$, but $m_{J,\text{ES}} = \pm 15/2$ yields an almost equally good result. We have tried a biaxial anisotropy term for the Cr^{III} ion; however, it did not improve the fits and resulted in the same D_{Cr} value. In view of the small magnetic coupling j we have tested whether our model would also be consistent with pure Dy–Cr dipolar coupling. For this we have replaced the isotropic exchange coupling in eq 1 by an anisotropic coupling matrix with $(2j_{\text{dip}}, -j_{\text{dip}}, -j_{\text{dip}})$ on its diagonal and zeros otherwise. The new fit

result was $j_{\text{dip}} = 0.043 \text{ cm}^{-1}$, in good agreement with the calculated value of $j_{\text{dip,calc}} = 0.029 \text{ cm}^{-1}$ for **3**, using the Dy^{III}–Cr spatial separation of $r_{\text{Dy–Cr}} = 3.42 \text{ \AA}$ from the structural analysis and the isotropic g -factors given before and assuming a collinear orientation of the Dy and Cr easy magnetization axes. For comparison, the closest intercluster metal ion distances are approximately 9 \AA , meaning that intercluster dipolar interactions are negligible. The other fit parameters turned out to be identical to the case of isotropic j . Details of the calculation are given in the Experimental Section.

DISCUSSION

As mentioned in the Introduction, it is important to characterize 3d–4f exchange coupling for a systematic approach to the design of 3d–4f clusters. An accurate characterization solely based on SQUID measurements is likely to fail for clusters containing 4f ions with orbital contribution to the magnetic moment. XMCD has the power to resolve element-specific magnetization curves, which we have used here to overcome the above-mentioned difficulties in the understanding of the magnetism of 3d–4f clusters. In the following we will give qualitative arguments based on the XMCD data why the Dy–Cr magnetic coupling in **3** can only be very small. The magnetic moment of the Cr^{III} ion is smaller than the one of Dy^{III}; hence in the case of a hypothetical antiferromagnetic coupling and at small fields compared to the coupling the Dy moment would be parallel and the Cr moment antiparallel to the magnetic field. In contrast, at large enough fields this coupling would break up, and both moments would be parallel to the field, leading to a wiggle shape in the Cr magnetization curve as seen for example in ref 11b. Because this wiggle shape is absent in **3**, a conservative estimate of a lower bound for the hypothetical antiferromagnetic Dy–Cr coupling $j \geq -\mu_{\text{B}}g_{\text{Cr}}B_0/J_{\text{Dy,z}} = -0.13 \text{ cm}^{-1}$ can be obtained, with B_0 the field at which the Cr magnetic moment would flip its sign. Because no such wiggle shape is observed in the experiment, we have used a B_0 of 0.15 T . On the other hand, a significant ferromagnetic coupling is inconsistent with the data, too, because then the Cr magnetization curve close to zero field would be steeper than the paramagnetic one, the latter being indicated by the dashed line in Figure 4a. These qualitative arguments advocate that the absolute value of the magnetic coupling j is close to zero in agreement with the fitting results. As observed in the fits, simple dipolar coupling between Dy^{III} and Cr^{III} ions can fully account for the observed magnetic interaction, and its strength is consistent with the calculated values from the Dy–Cr spatial separation. Hence, there is essentially no magnetic exchange coupling mediated by the methoxide bridges. In the reported examples of Cr^{III}–Dy^{III} clusters or extended networks, the Cr–Dy exchange interaction appears to be weak and antiferromagnetic irrespective of the bridging ligand being fluoride, hydroxide or cyanide.²⁴ Even though so far there is no report on alkoxide-bridged Cr(III)–lanthanide clusters, our studies suggest that such bridges do not lead to an exception to these findings. The fitting result of the Cr^{III} uniaxial anisotropy $D_{\text{Cr}} = -1.7(1.0) \text{ cm}^{-1}$ appears large, but in view of the experimental uncertainty a value of $D_{\text{Cr}} \sim -1.0 \text{ cm}^{-1}$, which is very reasonable for Cr^{III}, is also compatible with the data. The obtained separation between ground-state doublet and first-excited doublet of $\delta = 57(21) \text{ cm}^{-1}$ is in excellent agreement with values reported in the literature.²³ Also, the m_j values of $\pm 13/2$ and $\pm 11/2$ for the ground-state doublet and the first-excited state, respectively, are in very good agreement with

these studies. Regarding the comparison of the magnetic moments obtained by SQUID magnetometry and XMCD, despite an excellent overall agreement we observe a slight deviation of the cluster magnetic moment from the sum of the element-specific magnetic moments on the order of a few percent as visible in Figure 4. This deviation may be due to the fact that a SQUID magnetometer probes the entire bulk magnetic moment whereas XMCD only detects the targeted elemental magnetic moments, and even after taking into account diamagnetic contributions, ligand spin polarization (as, e.g., seen in ref 11a) may give rise to the observed deviations between SQUID and XMCD measurements. Restricting the Hilbert space of the Dy^{III} ion to two Kramers doublets has the advantage that the whole ligand field is reduced to three parameters, which are the m_j values of the ground state and excited state and the separation δ . This avoids overparametrization; however, it implies that the model can only be used for low enough temperatures at which all other Kramers doublets can be neglected. This becomes obvious in Figure 5: Clearly, there is perfect agreement at the lowest temperatures; however, at elevated temperatures $T > 20 \text{ K}$ the model curve lies below the measurement. The influence of temperature can be rationalized using a simple two-state model with an energy separation of 60 cm^{-1} assuming a Boltzmann distribution of populations. Exemplarily, at 2 K the population of the excited-state amounts to a negligible 1.7×10^{-19} , whereas at 20 K it is 0.013 , and similar populations can be expected if further excited states close in energy were added. This leads to deviations in the few-percent range, which is indeed observed in the experimental data in Figure 5. To improve the model, other Kramers doublets could be added; however, such a model would again be prone to overparametrization.

CONCLUSIONS

We have synthesized a novel methoxide-bridged Cr^{III}–Dy^{III} dimer and performed a detailed magnetic study. The element-specific and cluster magnetization curves obtained from XMCD and SQUID magnetometry as well as the dc magnetic susceptibility were fitted using a spin-Hamiltonian model yielding excellent agreement with the data. The Dy^{III} and Cr^{III} ions are magnetically almost isolated from each other with an exchange coupling of $j = -0.04(3) \text{ cm}^{-1}$. Further analysis reveals that our observations are consistent with the presence of purely dipolar coupling between Dy^{III} and Cr^{III} ions, suggesting that the double-methoxide bridge does not play any role in mediating exchange coupling. Furthermore, we determine the ground-state doublet of the Dy^{III} ion to be $m_{j,\text{GS}} = \pm 13/2$ and the first-excited doublet is $m_{j,\text{ES}} = \pm 11/2$ with an energy separation of $\delta = 57(21) \text{ cm}^{-1}$. The Cr^{III} ion exhibits a uniaxial anisotropy $D_{\text{Cr}} = -1.7(1.0) \text{ cm}^{-1}$.

ASSOCIATED CONTENT

Supporting Information

Table of crystal data, elemental analysis results, powder diffractogram, and figures comparing XAS and XMCD spectra. This material is available free of charge via the Internet at <http://pubs.acs.org>.

AUTHOR INFORMATION

Corresponding Author

*E-mail: J.D., jan.dreiser@psi.ch; J.B., bendix@kiku.dk.

Notes

The authors declare no competing financial interest.

ACKNOWLEDGMENTS

We acknowledge M. Schmidt for technical support. Part of this work was performed at the X-Treme beamline of the Swiss Light Source, Paul Scherrer Institut, Villigen, Switzerland. We gratefully acknowledge financial support for the XMCD endstation from Ecole Polytechnique Fédérale de Lausanne and from the Swiss National Science Foundation.

REFERENCES

- (1) (a) Kahn, O. In *Molecular Magnetism*; Wiley-VCH: Weinheim, Germany, 1993. (b) Gatteschi, D.; Sessoli, R.; Villain, J. In *Molecular Nanomagnets*; Oxford University Press: Oxford, U.K., 2006.
- (2) (a) Leuenberger, M. N.; Loss, D. *Nature* **2001**, *410*, 789–793. (b) Bogani, L.; Wernsdorfer, W. *Nat. Mater.* **2008**, *7*, 179–186.
- (3) (a) Winpenny, R. E. P. *Chem. Soc. Rev.* **1998**, *27*, 447–452. (b) Benelli, C.; Gatteschi, D. *Chem. Rev.* **2002**, *102*, 2369–2388. (c) Sessoli, R.; Powell, A. K. *Coord. Chem. Rev.* **2009**, *253*, 2328–2341. (d) Andruh, M.; Costes, J.-P.; Diaz, C.; Gao, S. *Inorg. Chem.* **2009**, *48*, 3342–3359.
- (4) (a) Osa, S.; Kido, T.; Matsumoto, N.; Re, N.; Pochaba, A.; Mrozinski, J. *J. Am. Chem. Soc.* **2004**, *126*, 420–421. (b) Zaleski, C. M.; Depperman, E. C.; Kampf, J. W.; Kirk, M. L.; Pecoraro, V. L. *Angew. Chem., Int. Ed.* **2004**, *43*, 3912–3914. (c) Mishra, A.; Wernsdorfer, W.; Abboud, K. A.; Christou, G. *J. Am. Chem. Soc.* **2004**, *126*, 15648–15649. (d) Mori, F.; Ishida, T.; Nogami, T. *Polyhedron* **2005**, *24*, 2588–2592. (e) Costes, J.-P.; Dahan, F.; Wernsdorfer, W. *Inorg. Chem.* **2006**, *45*, 5–7. (f) Aronica, C.; Pilet, G.; Chastanet, G.; Wernsdorfer, W.; Jacquot, J.-F.; Luneau, D. *Angew. Chem., Int. Ed.* **2006**, *45*, 4659–4662. (g) Pointillart, F.; Bernot, K.; Sessoli, R.; Gatteschi, D. *Chem.—Eur. J.* **2007**, *13*, 1602–1609. (h) Mereacre, V.; Ako, A. M.; Clérac, R.; Wernsdorfer, W.; Hewitt, I. J.; Anson, C. E.; Powell, A. K. *Chem.—Eur. J.* **2008**, *14*, 3577–3584. (i) Schray, D.; Abbas, G.; Lan, Y.; Mereacre, V.; Sundt, A.; Dreiser, J.; Waldmann, O.; Kostakis, G.; Anson, C.; Powell, A. *Angew. Chem., Int. Ed.* **2010**, *49*, 5185–5188. (j) Holyńska, M.; Premuzic, D.; Jeon, I.-R.; Wernsdorfer, W.; Clerac, R.; Dehnen, S. *Chem.—Eur. J.* **2011**, *17*, 9605–9610.
- (5) (a) Klokishner, S. I.; Ostrovsky, S. M.; Reu, O. S.; Pali, A. V.; Tregenna-Piggott, P. L. W.; Brock-Nannestad, T.; Bendix, J.; Mutka, H. *J. Phys. Chem. C* **2009**, *113*, 8573–8582. (b) Ungur, L.; Chibotaru, L. F. *Phys. Chem. Chem. Phys.* **2011**, *13*, 20086–20090.
- (6) (a) Bünzli, J. C. G.; Pigué, C. *Chem. Rev.* **2002**, *102*, 1897–1928. (b) Rinehart, J. D.; Long, J. R. *Chem. Sci.* **2011**, *2*, 2078–2085. (c) Car, P.-E.; Perfetti, M.; Mannini, M.; Favre, A.; Caneschi, A.; Sessoli, R. *Chem. Commun.* **2011**, *47*, 3751–3753. (d) Cucinotta, G.; Perfetti, M.; Luzon, J.; Etienne, M.; Car, P.-E.; Caneschi, A.; Calvez, G.; Bernot, K.; Sessoli, R. *Angew. Chem., Int. Ed.* **2012**, *51*, 1606–1610.
- (7) (a) Kahn, M. L.; Sutter, J. P.; Golhen, S.; Guionneau, P.; Ouahab, L.; Kahn, O.; Chasseau, D. *J. Am. Chem. Soc.* **2000**, *122*, 3413–3421. (b) Lukens, W. W.; Walter, M. D. *Inorg. Chem.* **2010**, *49*, 4458–4465.
- (8) (a) Figuerola, A.; Tangoulis, V.; Sanakis, Y. *Chem. Phys.* **2007**, *334*, 204–215. (b) Okazawa, A.; Nogami, T.; Nojiri, H.; Ishida, T. *Inorg. Chem.* **2008**, *47*, 9763–9765. (c) Sorace, L.; Sangregorio, C.; Figuerola, A.; Benelli, C.; Gatteschi, D. *Chem.—Eur. J.* **2009**, *15*, 1377–1388.
- (9) (a) Güdel, H. U.; Furrer, A.; Blank, H. *Inorg. Chem.* **1990**, *29*, 4081–4084. (b) Aebersold, M. A.; Güdel, H. U.; Hauser, A.; Furrer, A.; Blank, H.; Kahn, R. *Phys. Rev. B* **1993**, *48*, 12723.
- (10) (a) van der Laan, G.; Thole, B. T. *Phys. Rev. B* **1991**, *43*, 13401–13411. (b) Stöhr, J. *J. Magn. Magn. Mater.* **1999**, *200*, 470–497. (c) Funk, T.; Deb, A.; George, S. J.; Wang, H.; Cramer, S. P. *Coord. Chem. Rev.* **2005**, *249*, 3–30.
- (11) (a) Hamamatsu, T.; Yabe, K.; Towatari, M.; Osa, S.; Matsumoto, N.; Re, N.; Pochaba, A.; Mrozinski, J.; Gallani, J.-L.; Barla, A.; Imperia, P.; Paulsen, C.; Kappler, J.-P. *Inorg. Chem.* **2007**, *46*, 4458–4468. (b) Dreiser, J.; Pedersen, K. S.; Piamonteze, C.; Rusponi, S.; Salman, Z.; Ali, Md. E.; Schau-Magnussen, M.; Thuesen, C. A.; Piligkos, S.; et al. *Chem. Sci.* **2012**, *3*, 1024–1032.
- (12) (a) Paulovic, J.; Cimpoesu, F.; Ferbinteanu, M.; Hirao, K. *J. Am. Chem. Soc.* **2004**, *126*, 3321–3331. (b) Rajaraman, G.; Totti, F.; Bencini, A.; Caneschi, A.; Sessoli, R.; Gatteschi, D. *Dalton Trans.* **2009**, 3153–3161. (c) Shimada, T.; Okazawa, A.; Kojima, N.; Yoshii, S.; Nojiri, H.; Ishida, T. *Inorg. Chem.* **2011**, *50*, 10555–10557.
- (13) (a) Evangelisti, M.; Brechin, E. K. *Dalton Trans.* **2010**, *39*, 4672–4676. (b) Sessoli, R. *Angew. Chem., Int. Ed.* **2012**, *51*, 43–45. (c) Evangelisti, M.; Roubeau, O.; Palacios, E.; Camón, A.; Hooper, T. N.; Brechin, E. K.; Alonso, J. *J. Angew. Chem., Int. Ed.* **2011**, *50*, 6606–6609. (d) Sharples, J. W.; Zheng, Y.-Z.; Tuna, F.; McInnes, E. J. L. *Chem. Commun.* **2011**, *47*, 7650–7652. (e) Zheng, Y.-Z.; Evangelisti, M.; Winpenny, R. E. P. *Angew. Chem., Int. Ed.* **2011**, *50*, 3692–3695.
- (14) (a) Birk, T.; Schau-Magnussen, M.; Weyhermüller, T.; Bendix, J. *Acta Crystallogr.* **2011**, *E67*, m1561–m1562. (b) Birk, T.; Pedersen, K. S.; Thuesen, C. A.; Weyhermüller, T.; Schau-Magnussen, M.; Piligkos, S.; Weihe, H.; Mossin, S.; Evangelisti, M.; Bendix, J. *Inorg. Chem.* **2012**, *51*, 5435–5443.
- (15) (a) Blagg, R. J.; Muryn, C. A.; McInnes, E. J. L.; Tuna, F.; Winpenny, R. E. P. *Angew. Chem., Int. Ed.* **2011**, *50*, 6530–6533. (b) Blagg, R. J.; Tuna, F.; McInnes, E. J. L.; Winpenny, R. E. P. *Chem. Commun.* **2011**, *47*, 10587–10589.
- (16) Piamonteze, C.; Flechsig, U.; Rusponi, S.; Dreiser, J.; Heidler, J.; Schmidt, M.; Wetter, R.; Schmidt, T.; Pruchova, H.; Krempasky, J.; Quitmann, C.; Brune, H.; Nolting, F. Submitted for publication.
- (17) Krempasky, J.; Flechsig, U.; Korhonen, T.; Zimoch, D.; Quitmann, C.; Nolting, F. *AIP Conf. Proc.* **2010**, *1234*, 705–708.
- (18) Lebedev, V. I.; Laikov, D. N. *Dokl. Math.* **1999**, *59*, 477.
- (19) (a) Perdih, F.; Demsar, A.; Pevec, A.; Petricek, S.; Leban, I.; Giester, G.; Sieler, J.; Roesky, H. W. *Polyhedron* **2001**, *20*, 1967–1971. (b) Pevec, A.; Mrak, M.; Demsar, A.; Petricek, S.; Roesky, H. W. *Polyhedron* **2003**, *22*, 575–579. (c) McRobbie, A.; Sarwar, A. R.; Yeninas, S.; Nowell, H.; Baker, M. L.; Allan, D.; Luban, M.; Muryn, C. A.; Pritchard, R. G.; Prozorov, R.; Timco, G.; Tuna, F.; Whitehead, G. F. S.; Winpenny, R. E. P. *Chem. Commun.* **2011**, *47*, 6251–6253.
- (20) (a) Murugesu, M.; Mishra, A.; Wernsdorfer, W.; Abboud, K. A.; Christou, G. *Polyhedron* **2006**, *25*, 613–625. (b) Lin, P.-H.; Korobkov, I.; Wernsdorfer, W.; Ungur, L.; Chibotaru, L. F.; Murugesu, M. *Eur. J. Inorg. Chem.* **2011**, 1535–1539. (c) Shiga, T.; Hoshino, N.; Nakano, M.; Nojiri, H.; Oshio, H. *Inorg. Chim. Acta* **2008**, *361*, 4113–4117. (d) Mishra, A.; Tasiopoulos, A. J.; Wernsdorfer, W.; Abboud, K. A.; Christou, G. *Inorg. Chem.* **2007**, *46*, 3105–3115. (e) Shiga, T.; Onuki, T.; Matsumoto, T.; Nojiri, H.; Newton, G. N.; Hoshono, N.; Oshio, H. *Chem. Commun.* **2009**, 3568–3570. (f) Mishra, A.; Wernsdorfer, W.; Abboud, K. A.; Christou, G. *J. Am. Chem. Soc.* **2004**, *126*, 15648–15649. (g) Murugesu, M.; Mishra, A.; Wernsdorfer, W.; Abboud, K. A.; Christou, G. *Polyhedron* **2006**, *25*, 613–625.
- (21) (a) Thole, B. T.; Carra, P.; Sette, F.; van der Laan, G. *Phys. Rev. Lett.* **1992**, *68*, 1943–1946. (b) Carra, P.; Thole, B. T.; Altarelli, M.; Wang, X. *Phys. Rev. Lett.* **1993**, *70*, 694–697. (c) Chen, C. T.; Idzerda, Y. U.; Lin, H.-J.; Smith, N. V.; Meigs, G.; Chaban, E.; Ho, G. H.; Pellegrin, E.; Sette, F. *Phys. Rev. Lett.* **1995**, *75*, 152–155.
- (22) (a) Powell, M. J. D.; Orbach, R. *Proc. Phys. Soc.* **1961**, *78*, 753–758. (b) Mookherji, A.; Chachra, S. P. *J. Phys. Chem. Solids* **1969**, *30*, 2399–2404.
- (23) (a) Ishikawa, N.; Sugita, M.; Okubo, T.; Tanaka, N.; Iino, T.; Kaizu, Y. *Inorg. Chem.* **2003**, *42*, 2440–2446. (b) Luzon, J.; Bernot, K.; Hewitt, I. J.; Anson, C. E.; Powell, A. K.; Sessoli, R. *Phys. Rev. Lett.* **2008**, *100*, 247205. (c) Bernot, K.; Luzon, J.; Bogani, L.; Etienne, M.; Sangregorio, C.; Shanmugam, M.; Caneschi, A.; Sessoli, R.; Gatteschi, D. *J. Am. Chem. Soc.* **2009**, *131*, 5573–5579.
- (24) (a) Estrader, M.; Ribas, J.; Tangoulis, V.; Solans, X.; Font-Bardia, M.; Maestro, M.; Diaz, C. *Inorg. Chem.* **2006**, *45*, 8239–8250. (b) Rinck, J.; Novitchi, G.; van den Heuvel, W.; Ungur, L.; Lan, Y.; Wernsdorfer, W.; Anson, C. E.; Chibotaru, L. F.; Powell, A. K. *Angew. Chem., Int. Ed.* **2010**, *49*, 7583–7587.

Supporting Information

XMCD Study of a Methoxide-Bridged Dy^{III}-Cr^{III} Cluster Obtained by Fluoride Abstraction from *cis*- $[\text{Cr}^{\text{III}}\text{F}_2(\text{phen})_2]^+$

Jan Dreiser,^{†} Kasper S. Pedersen,[‡] Torben Birk,[‡] Magnus Schau-Magnussen,[‡] Cinthia Piamonteze,[†] Stefano Rusponi,[¶] Thomas Weyhermüller,[#] Harald Brune,[¶] Frithjof Nolting,[†] and Jesper Bendix^{‡*}*

[†]Swiss Light Source, Paul Scherrer Institut CH-5232 Villigen PSI, Switzerland, [‡]Department of Chemistry, University of Copenhagen, DK-2100 Copenhagen, Denmark, [¶]Institute of Condensed Matter Physics, Ecole Polytechnique Fédérale de Lausanne, CH-1015 Lausanne, Switzerland, [#]Max Planck Institute for Bioinorganic Chemistry, D-45470 Mülheim an der Ruhr, Germany.

*Authors to whom correspondence should be addressed. Email: jan.dreiser@psi.ch, bendix@kiku.dk

Crystallographic information

	1	2	3
formula	(C ₂₆ H ₂₂ CrN ₈ NdO ₁₄)·2(CH ₄ O)	C ₂₆ H ₂₂ CrN ₈ O ₁₄ Tb·2.62(CH ₄ O)	C ₂₆ H ₂₂ CrDyN ₈ O ₁₄ ·2.73(CH ₄ O)
<i>M</i> _r /g mol ⁻¹	930.84	954.96	961.34
color, shape	Red-violet, transparent block	Red-violet, transparent block	Red-violet, transparent block
crystal size/mm	0.05 × 0.05 × 0.02	0.39 × 0.24 × 0.16	0.16 × 0.12 × 0.03
crystal system	Orthorhombic	Orthorhombic	Orthorhombic
space group	<i>Pbcn</i>	<i>Pbcn</i>	<i>Pbcn</i>
<i>T</i> /K	100	122	122
<i>a</i> /Å	20.439(4)	20.352(4)	20.361(11)
<i>b</i> /Å	10.379(2)	10.2351(9)	10.212(6)
<i>c</i> /Å	17.293(3)	17.276(3)	17.337(10)
<i>V</i> /Å ³	3668.5(12)	3598.6(11)	3605(4)
<i>Z</i>	4	4	4
ρ_{calc} /g cm ⁻³	1.685	1.763	1.771
<i>F</i> ₀₀₀	1864	1887	1897
μ (Mo <i>K</i> α)/mm ⁻¹	1.78	2.34	2.44
θ range/°	3.6–36.6	2.2–33.0	2.2–25.0
collected reflns	131233	175184	96887
unique reflns	8817	6783	3168
params/restraints	274/16	285/0	285/0
reflns (<i>I</i> > 2 σ (<i>I</i>))	6849	5142	2795
GoF	1.14	1.39	1.32
<i>R</i> ¹ (<i>I</i> > 2.00 σ (<i>I</i>))	0.036	0.038	0.063
<i>R</i> ¹ (all data)	0.0517	0.0571	0.0701
<i>wR</i> ² (all data)	0.103	0.098	0.156
max/min ($\Delta\rho$ /eÅ ⁻³)	1.71/–1.19	0.86/–1.12	0.84/–1.13

Table S1. Crystallographic data of 1–3.

Analysis of the by-product

Elemental analysis (C, H, N) of the white by-product yields: C: 1.28%, H: 0.57%, N: 2.03%. Figure S1 shows the powder diffractogram of the by-product. The origin of peak X is not known but the presence of only small amounts of C, H and N suggests that the main phase is DyF_3 which, to a large extent, is amorphous.

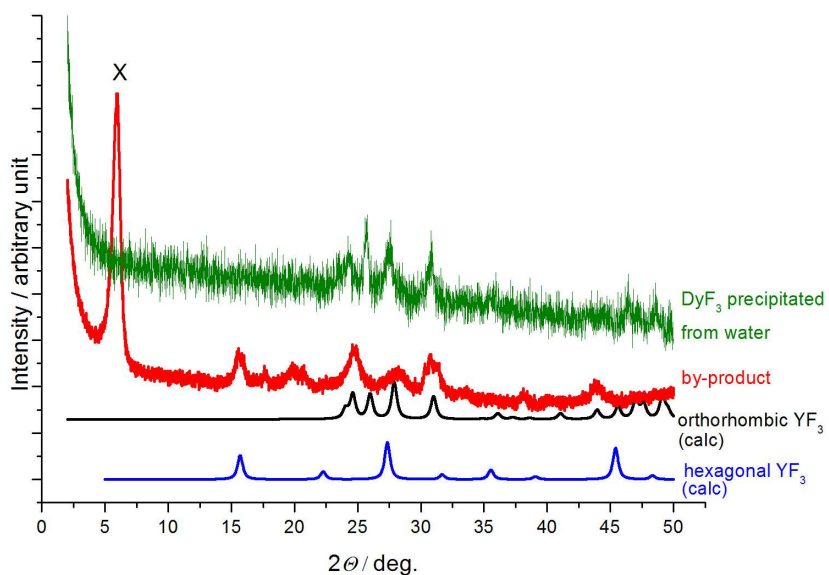


Figure S1. Powder diffractogram of the by-product (red). For comparison, the diffractogram of DyF_3 precipitated from water (green) and the simulated diffractograms of orthorhombic (black) and hexagonal (blue) YF_3 are shown. Data used in the simulations were obtained from the ICSD database, version July 2011.

Analysis of the X-ray spectra of $[\text{Cr}^{\text{III}}(\text{phen})_2(\mu\text{-MeO})_2\text{Dy}(\text{NO}_3)_4]$

The extraction of element-specific spin and orbital magnetic moments from polarization-dependent XAS has been carried out using the XMCD sum rules [1]. The quantities that enter are the integral over the entire X-ray absorption spectrum, the integral over the peak intensities of the L_2 and L_3 edges (for Cr) or of the M_4 and M_5 edges (for Dy), respectively, and the number of holes in the valence shell. While the sum rules can be applied in a straightforward manner to the Dy X-ray spectra, care has to be taken when treating the spectra recorded on the Cr^{III} ion. Here the L_2 and L_3 edges are not well separated, because of a relatively small spin-orbit coupling. In such a situation it has been shown that the sum rules can be subject to large errors. It has been demonstrated that as a remedy, a spin correction factor can be obtained from ligand-field multiplet calculations [2]. The values for the $\langle S_z \rangle$ expectation value found from sum rules then have to be corrected by this factor, defined as $\langle S_z \rangle = f_{\text{SC}} \cdot \langle S_{z,\text{SR}} \rangle$, where $\langle S_{z,\text{SR}} \rangle$ denotes the expectation value of the spin z component determined using sum rules. In a recent study we have performed ligand-field multiplet calculations to simulate the X-ray spectra around the Cr $L_{2,3}$ edges observed on a fluoride-bridged DyCrDy cluster [3]. In these studies we obtained a spin correction factor of $f_{\text{SC}} = 2.19$. Since the Cr $L_{2,3}$ X-ray spectra of the present system and those published in [3] are very similar as visible in Figure S2, we have used the same factor to correct the $\langle S_{z,\text{SR}} \rangle$ values of Cr.

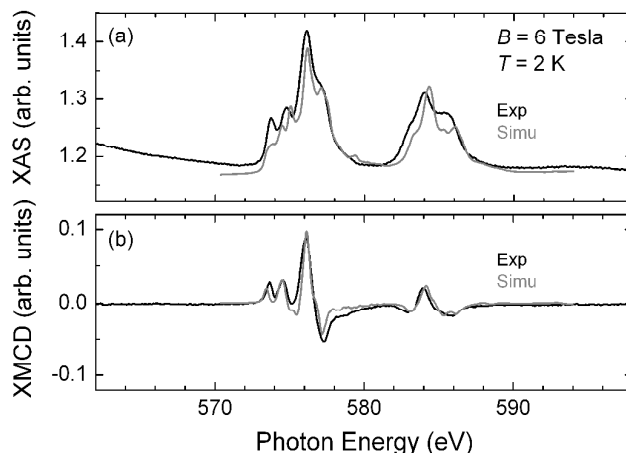


Figure S2. Comparison of experimental (this work) and simulated (from ref [3]) XAS and XMCD spectra. The spectra were recorded on compound **3** described in the main text.

An example for the integrals over the X-ray spectra is shown in Figure S3. In this particular case, the value of the integral over the absorption spectrum was 0.97, while we obtained 0.031 and -0.035 for the integrals over the XMCD at the L_3 and L_2 edges, respectively. Assuming a number of holes of $N_{\text{eff}} = 7$, these values yielded a total magnetic moment of $3.1 \mu_{\text{B}}$ in excellent agreement with the expected saturation value of the Cr^{III} ion of $3.0 \mu_{\text{B}}$.

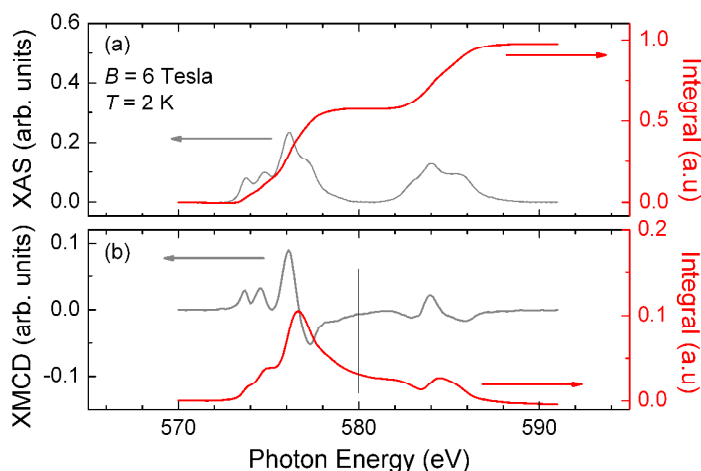


Figure S3. Example XAS and XMCD integrals around the Cr $L_{2,3}$ edges used for the sum rules calculations. The spectra were measured on compound **3** described in the main text.

References

-
- [1] Thole, B. T.; Carra, P.; Sette, F.; van der Laan, G. *Phys. Rev. Lett.* **1992**, *68*, 1943-1946; Carra, P.; Thole, B. T.; Altarelli, M.; Wang, X. *Phys. Rev. Lett.* **1993**, *70*, 694-697; Chen, C. T.; Idzerda, Y. U. ; Lin, H.-J. ; Smith, N. V.; Meigs, G.; Chaban, E.; Ho, G. H.; Pellegrin, E.; Sette, F. *Phys. Rev. Lett.* **1995**, *75*, 152-155.
- [2] Teramura, Y.; Tanaka, A.; Jo, T. *J. Phys. Soc. Jpn.* **1996**, *65*, 1053-1055; Goering, E. *Philos. Mag.* **2005**, *85*, 2895-2911; Piamonteze, C.; Miedema, P.; de Groot, F. M. F. *Phys. Rev. B* **2009**, *80*, 184410.
- [3] Dreiser, J.; Pedersen, K. S.; Piamonteze, C.; Rusponi, S.; Salman, Z.; Ali, M. E.; Schau-Magnussen, M.; Thuesen, C. A.; Piligkos, S.; Weihe, H.; Mutka, H.; Waldmann, O.; Oppeneer, P.; Bendix, J.; Nolting, F.; Brune, H.; *Chem. Sci.* **2012**, *3*, 1024-1032.